ROBUST ESTIMATION OF THE HEMODYNAMIC RESPONSE FUNCTION IN ASYNCHRONOUS MULTITASKS MULTISESSIONS EVENT-RELATED FMRI PARADIGMS

Philippe Ciuciu[†,¶], *Guillaume Marrelec*[‡,¶], *Jean-Baptiste Poline*[†,¶], *Jérôme Idier*[*], *Habib Benali*[‡,¶]

[†] SHFJ/CEA, 4 Pl. du Général Leclerc, 91 406 Orsay, France (ciuciu@shfj.cea.fr)
[‡] INSERM U494, CHU Pitié-Salpêtrière, 91 bd de l'Hôpital, 75634 Paris cedex 13, France
[*] L2S, SUPÉLEC, Plateau de Moulon 91192 Gif–sur–Yvette cedex, France
[¶] IFR 49, Neuroimagerie fonctionnelle, Paris, France

ABSTRACT

Hemodynamic Response Function (HRF) estimation in noisy functional Magnetic Resonance Imaging (fMRI) is essential for a better understanding of cerebral activations. Previous works have proposed robust non-parametric estimates of the HRF within a regularized framework [1, 2]. They are not adapted for event-related paradigms that are either *asynchronous* (in which the onsets of the conditions are not synchronized with the data), or designed with several kinds of trials, or with several sessions. In this paper, we extend [1, 2] to these three situations. We introduce temporal prior information on the underlying physiological process of the brain hemodynamic response to accurately estimate the HRF in a Bayesian framework. The proposed unsupervised approach is validated on both synthetic and real fMRI data.

1. INTRODUCTION

The end goal of activation detection in brain functional imaging experiments is to retrieve as much as possible the neuronal activity in response to cognitive or behavioral tasks [3]. However, the relation between this activity and the Blood Oxygen Level-Dependent (BOLD) response [4], measured with fMRI, is not completely understood [5, 6]. A first step towards a better quantification of the brain neuronal activity is therefore useful. It is currently done by modeling information transfer from reception to the stimulus to measurement of the BOLD signal, as a system characterized by its impulse response, the so-called HRF [7]. In this work, as well as in [7, 8, 9], we assume that the brain system is linear and time invariant (LTI). It has been shown that, although not perfect, this assumption is a tenable and useful approximation [8] as long as the inter-stimulus (ISI) interval does not decrease below about two seconds.

Whereas first contributions [7] were devoted to parametric estimation constraining the shape of the HRF, recent works [1, 2] have used a non-parametric framework to estimate *one* HRF in event-related paradigms. The use of these techniques has remained limited since they are not well-adapted to real fMRI data. We have developed a threefold extension. This contribution actually considers *asynchronous* event-related protocols, accounts for different trial types and integrates several fMRI sessions in the estimation. These generalizations are simultaneously addressed in Section 2 through a badly-conditioned observation model. In Section 3, we introduce temporal prior information on the HRFs in a Bayesian framework. The HRFs estimate is then defined as the Maximum *A Posteriori* (MAP). Section 4 illustrates the performances of our HRFs estimate on both synthetic and real data, the latter originated from a speech perception experiment.

2. MODELING THE CEREBRAL HEMODYNAMIC RESPONSE

In event-related protocols with synchronous ISI, the BOLD fMRI time course $(y_n)_{1\leq n\leq N}$ is measured at times $(t_n = nTR)_{1\leq n\leq N}$, TR being the repetition time, in any voxel of the brain after stimulating the subject with a fixed-delayed impulse signal $(x_n)_{1\leq n\leq N}$. The HRF is then modeled as the convolution kernel of a LTI system. In *asynchronous* experiments, the sampling frequency of the data is too low to match the onsets of the events with a small error. Accordingly, the HRF has to be estimated with a high (temporal) resolution model. To this end, let Δt be the sampling period defining a fine temporal grid on which the data and the trials of the stimulus $(x_t)_{t\geq t_0}$ can be put together:

$$y_{t_n} = \sum_{p=0}^{P} h_{p\Delta t}\, x_{t_n - p\Delta t} + b_{t_n} = \boldsymbol{x}_{t_n}^t \boldsymbol{h} + b_{t_n},\ \forall t_n, \quad (1)$$

with $\boldsymbol{x}_{t_n} = [x_{t_n}, x_{t_n-\Delta t}, \ldots, x_{t_n - P\Delta t}]^t \in \mathbb{R}^{P+1}$, and $\boldsymbol{h} = [h_0, h_{\Delta t}, \ldots, h_{P\Delta t}]^t$. b_n is the nth sample of a zero-mean Gaussian white noise process $\boldsymbol{b}$ of unknown variance $r_b > 0$, independent of $\boldsymbol{h}$.

0-7803-7584-X/02/$17.00 ©2002 IEEE

In present experiments, the fMRI raw data are contaminated by a low-frequency drift mainly due to physiological artifacts: breathing and cardiac pulses are aliased since the sampling frequency of the data is below Shannon's bound. A high-pass filter is generally used to remove those trends before estimating the HRF. In this study, we simultaneoulsy estimate the HRF and the trend with the following model

$$\boldsymbol{y} = \boldsymbol{X}\boldsymbol{h} + \boldsymbol{P}\boldsymbol{l} + \boldsymbol{b}, \tag{2}$$

where $\boldsymbol{y} = [y_{t_1}, \ldots, y_{t_N}]^t$, $\boldsymbol{X} = [\boldsymbol{x}_{t_1}, \ldots, \boldsymbol{x}_{t_N}]^t$ and $\boldsymbol{P} = [P_1, \ldots, P_Q]$ consists of functions (orthonormal) basis $P_q = [P_q(t_1), \ldots, P_q(t_N)]^t$ (*e.g.*, a discrete cosine transform). Scalar Q depends on the lowest frequency $f_{\min}$ attributable to the drift term. Matrix $\boldsymbol{P}$ can also take into account any covariate of no interest, supposed to influence the signal intensity in a linear way. Vector $\boldsymbol{l} \in \mathbb{R}^Q$ defines the unknown weighting coefficients of the basis functions.

We further extend this model to allow for a different HRF estimate for different trial types (*e.g.*, different stimuli or conditions). Let $(\boldsymbol{X}^{(m)})_{1 \leqslant m \leqslant M}$ be the different trial-dependent matrices, each of them being defined as the previous $\boldsymbol{X}$ matrix, and then suppose that the HRFs $\boldsymbol{h}_m$ add in a *linear* way. Such an extension requires to correctly define the over-sampling period Δt as the smallest sampling interval that allows to separate the two closest events, whatever their type. For the sake of simplicity, let us define

$$\boldsymbol{X} = [\boldsymbol{X}^{(1)} | \ldots | \boldsymbol{X}^{(M)}] \in \mathbb{R}^N \times \mathbb{R}^{MP}, \boldsymbol{h} = [\boldsymbol{h}_1^t, \ldots, \boldsymbol{h}_M^t]^t;$$

from which model (2) is able to cope with *asynchronous multitasks* paradigms.

Compared to the single trial asynchronous case, the current identification problem becomes much more undetermined: the number of data remains constant whereas the number of unknown parameters significantly increases (M usually varies between 2 and 6 and Q is typically around 10). On the other hand, during an fMRI experiment, several sessions of many trials each are generally acquired on each subject for experimental or cognitive reasons. Model (2) only suggests a session-dependent estimation of the HRFs. Since the HRF remains approximately constant as far as all the exogenous parameters (voxel, task, subject) are fixed, a straightforward extension consists in searching for *one* vector $\boldsymbol{h}$ from all the available fMRI times series $(\boldsymbol{y}_1, \ldots, \boldsymbol{y}_I$ of respective length N_i) with

$$(H): \ \boldsymbol{y}_i = \boldsymbol{X}_i\boldsymbol{h} + \boldsymbol{P}_i\boldsymbol{l}_i + \boldsymbol{b}_i, \text{ for } i \in \mathbb{N}_I^* = \{1, \ldots, I\},$$

where the stimuli and thus matrices $\boldsymbol{X}_i$ vary accross the sessions. Similarly, the physiological factors (cardiac and breathing rates) fluctuate throughout the sessions, so that different vectors $\boldsymbol{l}_i$ and scalars Q_i are involved in (H).

Assuming that times series $(\boldsymbol{b}_i)_{1 \leqslant i \leqslant I}$ independent and indentically distributed, the likelihood of model (H) reads:

$$p(\mathbf{y} \,|\, \boldsymbol{h}, H; \boldsymbol{\theta}_0) = \prod_{i=1}^{I} p(\boldsymbol{y}_i \,|\, \boldsymbol{h}, H; \boldsymbol{l}_i, r_b)$$

$$= (2\pi r_b)^{-\sum_{i=1}^{I} N_i/2} \exp\left(-\sum_{i=1}^{I} \|\boldsymbol{y}_i - \boldsymbol{P}_i\boldsymbol{l}_i - \boldsymbol{X}_i\boldsymbol{h}\|^2 / 2r_b \right)$$

where $\mathbf{y} = [\boldsymbol{y}_1^t \,|\, \ldots \,|\, \boldsymbol{y}_I^t]^t$ and $\boldsymbol{\theta}_0 = [\boldsymbol{l}_1^t, \ldots, \boldsymbol{l}_I^t, r_b]$. The number of parameters remains still large so that least squares estimation is unreliable when $\boldsymbol{X}_i^t\boldsymbol{X}_i$ is ill-conditioned. The limit case, corresponding to the underdetermination of (2), can be reached if Δt is too low or M too large.

3. IDENTIFICATION OF THE HRFS

3.1. Prior information

Following [1, 2], we introduce temporal prior information within the Bayesian framework. Each HRF may be characterized by the following physiological features [5]:
(a) Its amplitude is close to zero at the first and end points.
(b) Its variations are smooth.
(c) Moreover, prior statistical independence is supposed between conditions and thus between HRFs.

Condition *(a)* is easily introduced by redefining vectors $\boldsymbol{h}_m$ and $\boldsymbol{x}_{i,t_n}^{(m)}$ for the ith session and all $n \in \mathbb{N}_{N_i}^*$

$$\begin{aligned}
\boldsymbol{h}_m &\triangleq [h_{m,\Delta t}, \ldots, h_{m,(P-1)\Delta t}]^t \in \mathbb{R}^{P-1}, \\
\boldsymbol{x}_{i,t_n}^{(m)} &\triangleq [x_{i,t_n-\Delta t}^{(m)}, \ldots, x_{i,t_n-(P-1)\Delta t}^{(m)}]^t \in \mathbb{R}^{P-1}, \\
\boldsymbol{X}_i^{(m)} &\triangleq [\boldsymbol{x}_{i,t_1}^{(m)}, \ldots, \boldsymbol{x}_{i,t_N}^{(m)}]^t \in \mathbb{R}^{N_i} \times \mathbb{R}^{P-1}.
\end{aligned}$$

Then, the likelihood of model (H) remains unchanged with $\boldsymbol{h} = [\boldsymbol{h}_1^t, \ldots, \boldsymbol{h}_M^t]^t$ and $\boldsymbol{X}_i = [\boldsymbol{X}_i^{(1)} \,|\, \ldots \,|\, \boldsymbol{X}_i^{(M)}]$.

Quantification of condition *(b)* is achieved by setting a Gaussian probability density function (pdf) $\mathcal{N}(0, r_m\boldsymbol{R})$ for each HRF $\boldsymbol{h}_m$. The prior covariance matrix $\boldsymbol{R}$ has been defined according to $\boldsymbol{R} = (\boldsymbol{D}_2^t\boldsymbol{D}_2)^{-1}$ where the second-order finite differences matrix $\boldsymbol{D}_2$ has been truncated to respect constraint*(a)*. Condition *(c)* is then taken into account by the following pdf:

$$p(\boldsymbol{h}; \boldsymbol{R}, \boldsymbol{\theta}_1) = \prod_{m=1}^{M} p(\boldsymbol{h}_m; \boldsymbol{R}, r_m) \tag{3}$$

where $\boldsymbol{\theta}_1 = [r_1, \ldots, r_M] \in \mathbb{R}^M$ stands for the hyperparameters vector of the prior model. Introduction of different prior variances for different HRFs allows to model specific dynamics for each condition.

3.2. Posterior distribution

Combining the likelihood and the prior (3) with Bayes rule we get the Gaussian posterior distribution of $\boldsymbol{h}$, $\mathcal{N}(\widehat{\boldsymbol{h}}^{\text{MAP}}, \boldsymbol{\Sigma})$,

from which we derive the MAP estimate for the HRFs:

$$\widehat{h}^{\mathrm{MAP}} = \frac{\Sigma}{r_b} \sum_{i=1}^{I} \boldsymbol{X}_i^{\mathrm{t}} \left(\boldsymbol{y}_i - \boldsymbol{P}_i \boldsymbol{l}_i\right)$$

with $\Sigma^{-1} = \sum_{i=1}^{I} \boldsymbol{X}_i^{\mathrm{t}} \boldsymbol{X}_i / r_b + \boldsymbol{R}_H^{-1}$ and

$$\boldsymbol{R}_H = \mathrm{diag}\left[r_1 \boldsymbol{R}, r_2 \boldsymbol{R}, \ldots, r_M \boldsymbol{R}\right].$$

Uncertainty measures of $\widehat{h}^{\mathrm{MAP}}$ are straightforward to compute. As we would like to assess the error made on the components of each $\boldsymbol{h}_m$ separately, we focus on the marginal posterior pdf of $\boldsymbol{h}_m$. As expected, the latter is $\mathcal{N}(\widehat{\boldsymbol{h}}_m^{\mathrm{MAP}}, \boldsymbol{\Sigma}_m)$-distributed with $\boldsymbol{\Sigma}_m$, the mth diagonal block of $\boldsymbol{\Sigma}$. Then, the marginal error bars derive from the standard deviations $\sigma_{m,p}$, given by the main diagonal of $\boldsymbol{\Sigma}_m$.

3.3. Hyperparameters estimation

Following [1], we select the hyperparameters $\boldsymbol{\theta} = [\boldsymbol{\theta}_0^{\mathrm{t}}, \boldsymbol{\theta}_1^{\mathrm{t}}]^{\mathrm{t}}$ by maximization of their likelihood $p(\mathbf{y}|H;\boldsymbol{\theta})$. The Maximum-Likelihood (ML) estimator $\widehat{\boldsymbol{\theta}}^{\mathrm{ML}}$ of $\boldsymbol{\theta}$ minimizes [10]

$$\log\det(\Upsilon) + (\mathbf{y} - \mathbb{P}\mathbf{l})^{\mathrm{t}} \Upsilon^{-1} (\mathbf{y} - \mathbb{P}\mathbf{l}) \qquad (4)$$

with $\{\mathbb{X}, \mathbf{l}, \mathbb{P}\} \triangleq [\{\boldsymbol{X}, \boldsymbol{l}, \boldsymbol{P}\}_1^{\mathrm{t}} | \ldots | \{\boldsymbol{X}, \boldsymbol{l}, \boldsymbol{P}\}_I^{\mathrm{t}}]^{\mathrm{t}}$ and $\Upsilon = r_b \boldsymbol{I}_N + \mathbb{X} \boldsymbol{R}_H^{-1} \mathbb{X}^{\mathrm{t}}$. Computation of $\widehat{\boldsymbol{\theta}}^{\mathrm{ML}}$ is a complicated nonlinear optimization problem, since $\log\det(\Upsilon)$ is non-quadratic and $\log p(\mathbf{y}|H;\boldsymbol{\theta})$ is not concave with respect to $\boldsymbol{\theta}$. To avoid direct optimization of (4), we have adapted to the present context an Expectation Conditional Maximization algorithm [10] to compute a stationary point of $p(\mathbf{y}|H;\boldsymbol{\theta})$, *i.e.*, a local minimizer of (4).

4. VALIDATIONS

4.1. Simulation results

This part mainly focuses on the successive improvements supplied by the ability to take the drift and several sessions into account with model (H). Simulated data sets have been generated using realistic parameters.

For each session, we have first simulated a *random intermixed* sequence of indexes coding for two different event types ($M = 2$). Each index corresponds to a specific stimulus. The ISIs between successive trials are random and follow a uniform distribution on [2.5, 3.5]. The onsets of the trials are put together on the same temporal grid using $\delta t = 0.5$ s for sampling period. Each binary time series coupled to each stimulus is then convolved with a specific HRF, $\boldsymbol{h}_1$ or $\boldsymbol{h}_2$ (used by the SPM99 toolbox[1]), whose exact shapes are depicted in Fig. 1(a). Clearly, $\boldsymbol{h}_2$ is more peaked than $\boldsymbol{h}_1$ and has smaller dispersion. A white Gaussian noise ($r_b = 0.08$) and a $\mathcal{N}(\mathbf{0}_{Q_i}, \boldsymbol{I}_{Q_i})$-distributed low-frequency drift, whose cut-off-period varies from 50 to 70 s accross sessions, have been added. The data are then obtained after undersampling the sequences at $F = \lfloor TR/\delta t \rfloor$ rate, the inter-scan interval being $TR = 2$ s. Fig. 1(c) illustrates the gain brought by modeling a drift component in terms of accuracy on the HRFs estimate, compared to Fig. 1(b). Fig. 1(d) shows that more accurate and robust results are provided with model (H). Assuming stability of the HRFs accross sessions actually allows to increase the signal-to-noise ratio and leads to a significant bias reduction and a slight variance decrease.

The difference between Figs. 1(d)-(e) relies on the assumption on the dynamics of the original HRFs: Fig. 1(d) is obtained with the same prior variance for $\boldsymbol{h}_1$ and $\boldsymbol{h}_2$, whereas Fig. 1(e) is computed with a specific variance r_m for each $\boldsymbol{h}_m$. Fig. 1(e) provides more accurate and robust results for both HRFs: $\widehat{\boldsymbol{h}}_1$ appears smoother and $\widehat{\boldsymbol{h}}_2$ more peaked, thus seems closer to the true HRFs, with smaller error bars.

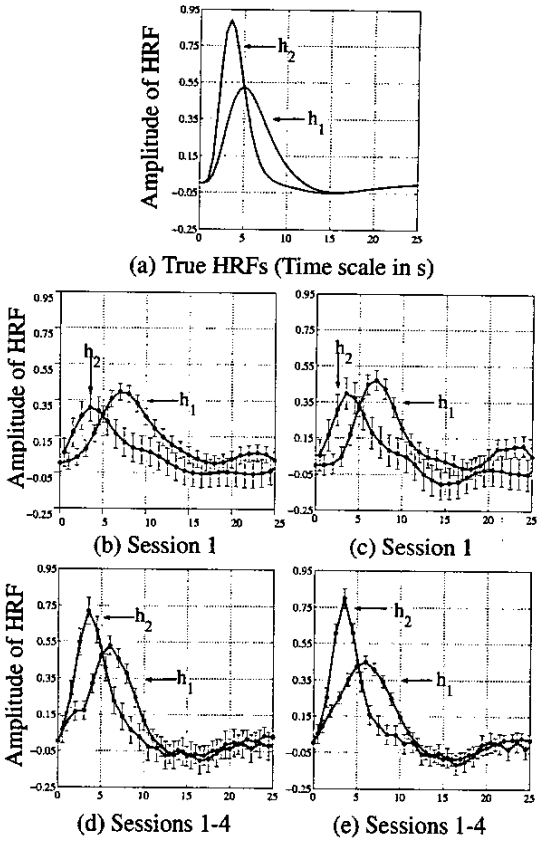

Fig. 1. HRFs estimated for no drift (b) *vs* drift modeling (c)-(e). Top row: single session estimation; bottom row: multi-sessions estimation.

[1] www.fil.ion.ucl.ac.uk/spm/spm99.html

4.2. Speech perception experiment

The method was applied to real data acquired in a speech discrimination experiment. In each trial, pseudo-words were delivered by pairs over headphones. The participant's task was to indicate whether he had perceived a difference between them. The trials belonged to one of three conditions ($M = 3$): 'Phonological' (h_1), 'Acoustic' (h_2) and 'Control' (h_3). In the 'Phonological' condition, the difference between the stimuli involved a contrast used to distinguish words in the language of the participant. In the 'Acoustic' condition, the contrast between the stimuli was not relevant in the language of the participant. In the 'Control' condition, the stimuli were exactly the same. Each trial lasted 2 s and was followed by the acquisition of one whole brain volume for 1.3 s using an EPI sequence; the TR was therefore 3.3 s. The experiment consisted of six sessions ($I = 6$) of one hundred trials each ($N_i = 100$).

Fig. 2 shows the HRFs estimates in three different voxels from the left superior temporal gyrus of one participant. These results have been obtained from model (H). Fig. 2(a) proves that the stimuli elicited very similar responses in Heschel gyrus (primary auditory cortex, V_1). The two other voxels are located in the planum temporale. Fig. 2(b) shows for V_2 that there is differential treatment when the stimuli differed, regardless of the type of difference (phonological or acoustic). By contrast, Fig. 2(c) shows a specific increment for phonological contrasts (speech processing).

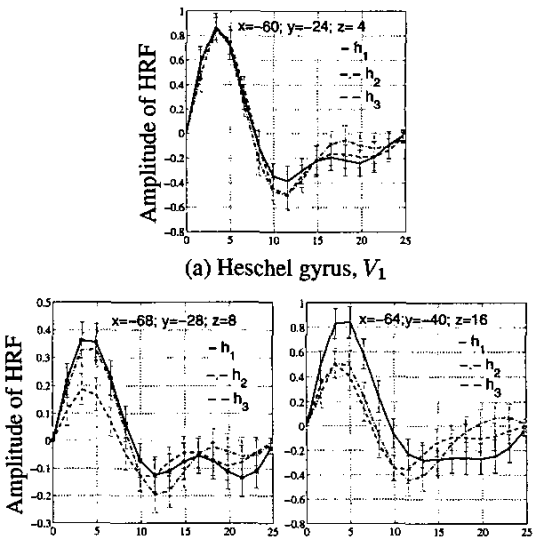

(a) Heschel gyrus, V_1

(b) Planum temporale, V_2 (c) Planum temporale, V_3

Fig. 2. Real data originated from a speech perception experiment. HRFs estimated from six sessions in the left superior temporal gyrus. 'Phonological', 'Acoustic' and 'Control' conditions are coupled with h_1, h_2, h_3, respectively.

5. CONCLUSION

In this paper, we have described and tested a general method for estimating the hemodynamic response function in fMRI data. The method is general enough to deal with all specific features of fMRI data. To our knowledge, this work presents the most comprehensive robust non-parametric estimation of the fMRI brain response to a task or a stimulus. Finally, this approach enables the detection of subtle differences between the HRFs estimated for different stimuli within the same brain region.

6. REFERENCES

[1] C. Goutte, F. A. Nielsen, and L. K. Hansen, "Modeling the haemodynamic response in fMRI using smooth filters," *IEEE Trans. Medical Imaging*, vol. 19, no. 12, pp. 1188–1201, Dec. 2000.

[2] G. Marrelec, H. Benali, P. Ciuciu, and J.-B. Poline, "Bayesian estimation of the hemodynamic response function in functional MRI," in *Bayesian Inference and Maximum Entropy Methods*, Robert Fry, Ed., Baltimore, MD, Aug. 2001, MaxEnt Workshops.

[3] P. A. Bandettini, A. Jesmanowicz, E. C. Wong, and J. S. Hyde, "Processing strategies for time-course data sets in functional mri of the human brain," *Magn. Reson. Med.*, vol. 30, pp. 161–173, 1993.

[4] S. Ogawa, T. Lee, A. Kay, and D. Tank, "Brain magnetic resonance imaging with contrast dependent on blood oxygenation," *Proc. Natl. Acad. Sci. USA*, vol. 87, no. 24, pp. 9868–9872, 1990.

[5] R. Buxton and L. Frank, "A model for the coupling between cerebral blood flow and oxygen metabolism during neural stimulation," *J. Cereb. Blood Flow Metab.*, vol. 17, no. 1, pp. 64–72, 1997.

[6] N. K. Logothetis, J. Pauls, M. Augath, T. Trinath, and A. Oeltermann, "Neurophysiological investigation of the basis of the fMRI signal," *Nature*, vol. 412, no. 6843, pp. 150–157, July, 12 2001.

[7] K. J. Friston, "Statistical parametric mapping," in *Functional Neuroimaging : Technical Foundations*, R.W. Thatcher, M. Hallet, T. Zeffiro, E.R. John, and M. Huerta, Eds., 1994, pp. 79–93.

[8] G. H. Glover, "Deconvolution of impulse response in event-related BOLD fMRI," *Neuroimage*, vol. 9, pp. 416–429, 1999.

[9] C. Gössl, L. Fahrmeir, and D. P. Auer, "Bayesian modeling of the hemodynamic response function in BOLD fMRI," *Neuroimage*, vol. 14, pp. 140–148, 2001.

[10] P. Ciuciu, J.-B. Poline, G. Marrelec, J. Idier, and H. Benali, "Robust estimation of the hemodynamic response function in asynchronous multitasks multiblocks event-related fMRI paradigms," Tech. Rep., SHFJ/CEA, , France, Dec. 2001.